



## Computations of effective moduli for microcracked materials : a boundary element approach

V. Renaud, D. Kondo, J.P. Henry

*Mechanics Laboratory of Lille (URA 1441 CNRS) University of Lille, F-59655 Villeneuve d'Ascq, France*

*Received 15 July 1995; accepted 31 August 1995*

### Abstract

---

The paper deals with a computational investigation of effective moduli of brittle materials weakened by microcracks. The study is based on a suitable adaptation of an indirect boundary element method, namely the displacement discontinuity method. Various aspects of microcracks size and orientation are investigated. For tensile loading (open cracks), the numerical results show good agreement with the classical non-interacting cracks approximation. Comparisons with some not fully random configurations are also presented. When crack – boundary interactions are taken into account, the results agree rather well with the differential approximation, but calculations under compressive loadings are much more complicated because of friction and sliding on crack faces, so an iterative algorithm for sliding and frictional cracks is used. The effective compliance in this case shows very little increase compared with the case of tensile loadings. Comparisons with some theoretical approximations are presented.

---

### 1. Introduction

Continuum damage mechanics (CDM) has become a suitable framework for the study of non-linear response of large class of materials such as concrete, rocks or ceramics. In the CDM field, the elastic parameters are assumed to be affected by pre-existing or growing microcracks. Macroscopic phenomenological approaches have been proposed for modeling this degradation process (see Ref. [15] for a complete review). Micromechanical modeling of cracked solids has also been the subject of recent works [e.g. 11,16,21]. The determination of effective stiffness for bodies containing microdefects appears through such studies as one of the fundamental aspects of

micromechanical modeling. This subject is usually treated from various theoretical standpoints.

In the non-interacting or dilute concentration approximation, microcracks are assumed to be isolated in the initial medium (Taylor model). The self-consistent method consists in the calculation of crack opening displacements (COD) for microcracks embedded in the unknown effective medium [3]. Interactions between microcracks are approximately taken into account through this assumption. The differential scheme is similar to the self-consistent one but interactions are considered through an incremental increase of crack density [8]. Although all these methods provide accurate approximation for low crack densities, they lead to some non-negligible differences in the case of moderate and strong densities. The

essential reason is that, when the density increases, microcracks become very close and their spatial locations (interactions) must play an important role on the overall properties. Kachanov [13] has used a superposition technique (or pseudo-tractions method) for such study. Recently, Ju and Tseng [12] have developed a statistical method which seems to give promising results. In general, however, it appears that the development of a suitable computing tool for treating elastic media with multiple interacting microcracks is of great interest. The displacement discontinuity method (DDM), originally developed by Crouch [6], was retained. In DDM (a plane strain boundary element method), each crack is simply represented by rectilinear segments on which the vector of displacement discontinuities is constant. Moreover this method can be applied to the complicated case of compressive loadings where microcracks can be closed and subjected to friction (see Ref. [10]). The outline of this paper is as follows. After a brief presentation of some theoretical approximations, we describe the displacement discontinuity method (DDM) and its adaptation for the present study. Afterwards, results for tensile loadings, i.e. open cracks, will be presented. Various aspects concerning microcrack size or orientation will be investigated. Special attention will be paid to microcrack – boundary interaction effects. The last section presents some significant results for compressive loadings.

## 2. Theoretical and numerical aspects for elastic moduli of cracked media

### 2.1. Theoretical models

In the last decades, the question of effective moduli for microcracked media has focused attention of several researchers (see Ref. [14]). Consider a representative volume element (RVE)  $V$  [9] which contains a set of distributed microcracks. The average strain tensor of the RVE is defined as,  $\bar{\epsilon} = \bar{\epsilon}^e + \bar{\epsilon}^*$ , where  $\bar{\epsilon}^e$  and  $\bar{\epsilon}^*$  are respectively the elastic and the

damage-induced strains. Similarly, the effective compliance is defined as  $\bar{S} = \bar{S}^0 + \bar{S}^*$ , where  $\bar{S}^0$  and  $\bar{S}^*$  are respectively the elastic and the damage-induced compliance. This effective compliance relates the average strain to the average stress  $\bar{\sigma}$  by :

$$\bar{\epsilon} = \bar{S} \bar{\sigma} \quad (1)$$

When stress boundary conditions are imposed on the RVE,  $\bar{\sigma}$  is equal to the remote applied stress. In two-dimensional analysis, the inelastic part of strains are then defined as (see [10,14;18,20]) :

$$\bar{\epsilon}_{ij}^* = \frac{1}{A} \sum_k \left[ \int_{l^{(k)}} (D_i n_j + D_j n_i) dl \right]^{(k)} \quad (2)$$

The vector  $D^{(k)}$  represents the crack opening displacement on the  $k$  th microcrack;  $n^{(k)}$  is the unit outward normal vector of the  $k$  th microcrack whose length is  $2l^{(k)}$ ,  $A$  represents the area of the RVE. From this formula it appears that in order to determine effective compliance one needs to evaluate the COD on all microcracks. The main difficulty in such a calculation is to find the solution (second Green tensor) of the elastic problem for a solid with many interacting microcracks. The simplest way to avoid it is to neglect the microcrack interactions (Taylor model), but in the case of moderate or high density it is necessary to take microcrack interactions into account. Several theoretical approximations exist for elastic media with interacting microcracks. The self-consistent methods (SCM) due to Hill and developed for cracked solids by Budiansky and O'Connell [3] considers that defects are embedded in the unknown effective material. The key parameter for such a study is the crack density  $\rho$  defined in two-dimensional problems as :

$$\rho = \frac{1}{A} \sum_k l^{(k)^2} \quad (3)$$

The classical formulation of the SCM leads to a finite critical value for the density [3] ; this is a physically unacceptable result. An improvement of the SCM, proposed by Christensen and Lo [4] is known as the three-phase model or the generalized self-consistent method. Another simpler improvement is the differential scheme (DIF) which assumes also that microcracks are embedded in the unknown effective

medium, but the crack density is increased in an incremental manner. Thus, the elastic moduli are calculated for each increment  $d\rho$  by resolution of differential equations [8,9,14,19]. An excellent summary of the main results given by the different schemes for microcracked materials can be found in the review paper by Kachanov [14]. Since all these theoretical approximations give very different results for moderate and strong densities up to 0.4, the objective of this work is to investigate interaction effects through numerical simulations.

## 2.2. Displacement discontinuity method for solids containing multiple cracks

The numerical method used for the study is an adaptation of the two-dimensional displacement discontinuity method (DDM) originally proposed by Crouch [6] in plane strain. The domain is discretized by a finite number of elements with unknown displacement discontinuities. Let us first define a straight crack line  $\Gamma$  in an infinite domain (Fig. 1).

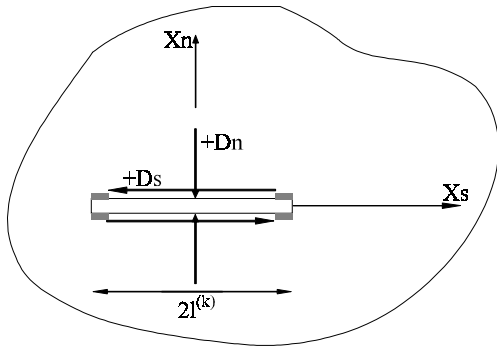


Fig. 1. Infinite medium with a crack.  $D_s$  and  $D_n$  are respectively the shear and normal COD.

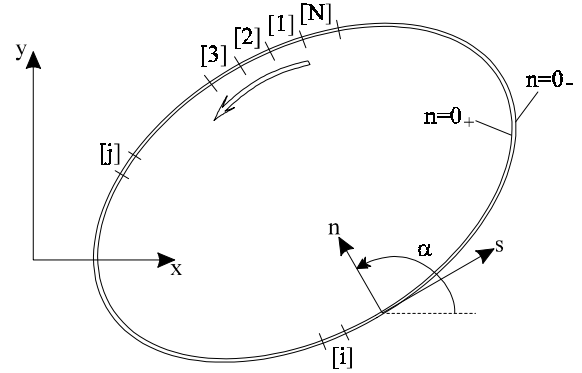


Fig. 2. Discretization of a finite medium in DDM.

The two displacement discontinuities are defined in all points of  $\Gamma$  as:

$$D_i = u_i(x_1, 0_-) - u_i(x_1, 0_+) \quad i = n, s. \quad (4)$$

The elastic solution (displacements and stresses field at any point  $x$  of the medium) of this problem can be written as follows (see for example [7,17,22]) :

$$U_i(x) = \int_{\Gamma} A_{ij}(x, \zeta) D_j(\zeta) d\Gamma \quad (5)$$

$A_{ij}$  is known as the fundamental solution associated with the application of a unit discontinuity displacement  $D_j$ , imposed in the direction  $j$  at point  $\zeta$  of the crack face. In two-dimensional elasticity  $A_{ij}$  can be expressed as follows (see e.g. [22]) :

$$A_{ij} = A_{ikn}(x, \zeta) = \frac{-1}{4\pi(1-\nu)} \left[ \frac{1-2\nu}{r^2} (y_i \delta_{kn} - y_n \delta_{ki} - y_k \delta_{in}) - \frac{2y_i y_k y_n}{r^4} \right] \quad (6)$$

In this expression  $n$  represents the unit normal direction of the crack;  $k = n$  when  $j$  corresponds to the normal discontinuity ; otherwise  $k = s$ .  $y_i$  and  $r$  are defined by :  $y_i = X_i - \zeta_i$  and  $r^2 = y_i y_i$ .  $\delta_{ik}$  is the Kronecker symbol. By differentiation of Eq. (6), one can evaluate  $\epsilon_{ij}(x)$  and then  $\sigma_{ij}(x)$ . The generalization to boundary value

problems is easy and consists of describing the frontier of the considered solid by  $N$  rectilinear elements and superposing the effects of these (Fig. 2). Let us denote now  $D_n^j$  and  $D_s^j$  respectively the normal and shear displacement discontinuities of the  $j$ th element (represented by one node). After some lengthy calculations which require frame transformation (between global and local coordinates) and analytical calculations of integrals, the method leads to the following linear algebraic system [7] :

$$\sum_{j=1}^N C_{ss}^{ij} D_s^j + C_{sn}^{ij} D_n^j = b_s^i$$

$$\sum_{j=1}^N C_{ns}^{ij} D_n^j + C_{nn}^{ij} D_s^j = b_n^i \quad \text{for } i = 1 \text{ to } N. \quad (7)$$

The vector  $b$  represents the boundary conditions (stresses or displacements) ;  $C$  is a non-symmetric influence coefficients matrix which contains four elementary matrices. For example  $C_{sn}$  is associated with the influence of a normal COD on shear stress or displacements.  $C$  depends on the elastic properties and the geometry of microcracks. The geometrical dependence allows interaction to be included since it is directly related to the relative spatial configurations of microdefects. Resolution of the system (7) gives the

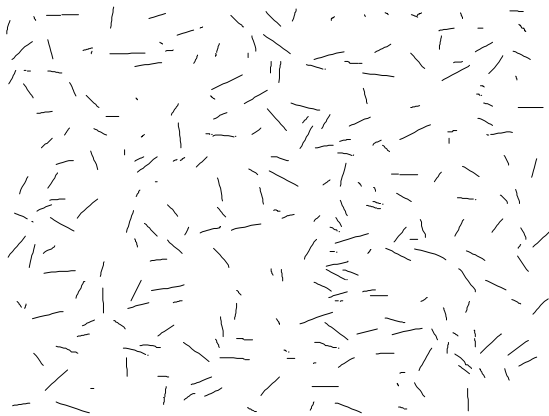


Fig. 3. Example of an array of randomly oriented cracks ( $p = 0.1$ ).

unknown COD  $D_n^j$  and  $D_s^j$  for all elements. Stresses and displacement field at any point of the medium can

then be determined by summation of the effects of all elements. It must be noted that there is no physical significance of the discontinuities at the frontier of the domain, but, in the case of a microcrack element,  $D_n^j$  and  $D_s^j$  represent well the average value of crack opening displacements which are needed for the effective moduli calculation. This is one of the greatest advantages of the DDM over other methods like the superposition technique [13]. The DDM is adapted in this work for solids containing multiple interacting cracks. A generator is built, which allows the desired random or non-random microcrack population to be constructed. The parameters of this automatic generation are the sizes, orientations and locations of the microcracks. For all simulations, microcrack intersections are prohibited. This was achieved by checking new generated microdefects. With such a condition, the centers of the cracks cannot be considered as uncorrelated, but it is expected that this limitation will not have a great influence on the trends of the numerical results on average (see also Ref. [14]).

### 3. Computer experiments for open microcracks

#### 3.1. Randomly distributed microcracks

Computations were conducted on a square domain of unit area  $A$  (Fig. 3). First simulations concern the case of randomly located and orientated microcracks. In order to separate crack – crack interactions and crack – boundary interaction effects, two types of simulations are performed.

##### 3.1.1. Simulations without microcrack – boundary interaction effects

These simulations are done by placing stress boundary conditions at infinity. For a statistical realization (one density  $\rho$ ), microcrack sizes were kept constant. The density parameter  $\rho$  (see Eq. (3)) is increased by increasing the number and/or size of microcracks. The numerical results are shown in Fig. 4. Each point of this figure represents a mean value of two

computations done in the horizontal and vertical directions. In fact, the two results are very close, proving the good accuracy of the method. Comparisons are done with non-interacting cracks (NIC) SCM and DIF results. We observe that our numerical results are in agreement with the non-interacting cracks approximation for a wide range of densities. This is in accordance with recent results obtained by Kachanov [14] or Bertaud et al. [2] who used the numerical pseudo-tractions method. Such results can be interpreted as a cancellation of the two competing effects (amplification and shielding) which rise from the interactions when microcracks are randomly distributed in space.

In order to check the relevance of crack density as a fundamental parameter, we have also carried out simulations with random crack size (in every realization). The microcrack size is considered to vary in average between a minimum value  $l_{\min}$  and a maximum value equal on average to  $10 l_{\min}$ . The corresponding results are shown in Fig. 5 and also lead to agreements with the NIC approximation. These results indicate that, even for microcracks with very different sizes, interaction effects also cancel because of randomness of the spatial distribution.

### 3.1.2. Effects of microcrack – boundary interactions

The sample boundary effects are also numerically investigated. The frontier of the area  $A$  is now discretized and the preceding microcrack distributions are used. Fig. 6 shows comparisons with the theoretical methods. One can note a clear difference with the preceding results. The numerical values are rather in agreement with the differential approximation. These results suggest that interaction effects cannot be neglected for the practical case of a finite domain.

### 3.2. Case of parallel cracks

The study of parallel microcracks distribution is of practical interest since under tensile loadings, the most

open microcracks are normal to the load direction. Simulations are conducted on microcracks array shown for example in Fig. 7. The variation of the effective modulus (Fig. 8) shows that the shielding effect of microcrack interactions is more pronounced here than in the case of randomly oriented cracks.

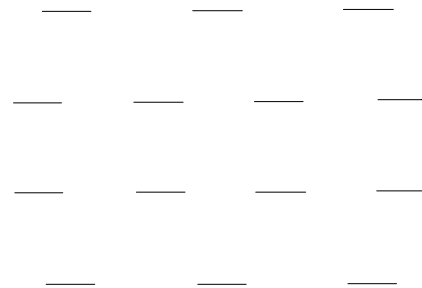


Fig. 7. Example of parallel microcrack array.

Moreover, the decrease of the modulus for the parallel microcracks distribution is more pronounced than for the random distribution. Finally we note that the numerical results again coincide with the NIC approximation. When microcrack – boundary interactions are considered the results show also good agreement with the differential method (Fig. 9).

## 4. Case of compressive loadings

Under compression, interactions become much more complex because of crack closure and sliding on crack faces. Hori and Nemat-Nasser [10] have studied in the framework of SCM the stress – induced anisotropy due to frictional sliding of microcracks. Because of theoretical difficulties, the necessity of computer experiments appears here to be of primary interest and may allow the study of a large class of problems.

### 4.1. Numerical treatment of closed cracks by DDM

In the numerical simulations, cracks are prescribed to not overlap (non-interpenetration of crack faces). This condition, classically known as Signorini's

condition, implies in the DDM that the normal COD  $D_n$  cannot be strictly positive. Let us denote by  $\sigma_n$  and  $\sigma_s$  respectively the normal and tangential stresses associated with a microcrack.

*Hypothesis : sliding is assumed possible for closed microcracks. Coulomb's friction law was retained for this study.*

Conditions on closed cracks are then :

no sliding :

if  $|\sigma_s| < \mu |\sigma_n|$  then  $D_n = D_s = 0$

friction with sliding :

if  $|\sigma_s| \geq \mu |\sigma_n|$  then  $|\sigma_s| = \mu |\sigma_n|$  ;

$D_n = 0$  and  $D_s \neq 0$

$\mu$  is the friction coefficient, equal to 0.5 in this study.

The numerical resolution was done by means of an iterative algorithm in which opening, closure and sliding on microcrack faces are checked. In a first approach, a Gauss – Seidel algorithm was used. Let us note, however, that a conjugate gradient approach (see Ref. [1]) can give similar results.

#### 4.2. Numerical results on effective compliance under uniaxial compression

Computations carried out in this section are done with constant microcrack length at each density level. The simulations correspond to stationary state of defects. No kinetic equations are investigated here. This is, however, a numerical aspect under investigation. The initial material is assumed to be isotropic with plane-strain conditions. In Voigt's two-dimensional notation, Hooke's law, which relates the effective strain  $\bar{\epsilon}_i$ , and stress  $\bar{\sigma}_j$ , ( $i, j = 1, 2, 3$ ), in a damaged elastic material is :  $\bar{\epsilon}_i = \bar{S}_{ij} \bar{\sigma}_j$  where  $\bar{S}$  is the effective compliance.

Initial elastic parameters are taken as :  $E_0 = 5 \times 10^4$  MPa,  $\nu_0 = 0.2$ . Thus, the undamaged compliance  $\bar{S}^0$  is given in plane-strain by :

$$\frac{1+\nu_0}{E_0} \begin{bmatrix} 1-\nu_0 & -\nu_0 & 0 \\ -\nu_0 & 1-\nu_0 & 0 \\ 0 & 0 & 2 \end{bmatrix}$$

with

$$\bar{S}_{11}^0 = \bar{S}_{22}^0 = 1.92 \times 10^{-5} \text{ MPa}^{-1}$$

$$\bar{S}_{12}^0 = \bar{S}_{21}^0 = -0.48 \times 10^{-5} \text{ MPa}^{-1}$$

$$\bar{S}_{33}^0 = 4.8 \times 10^{-5} \text{ MPa}^{-1}.$$

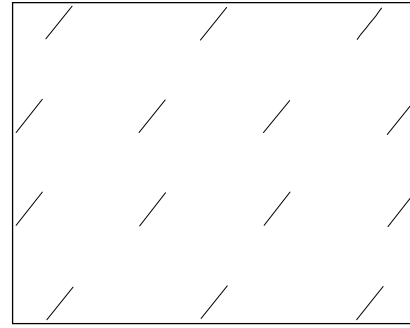


Fig 11. Example of parallel microcracks distribution tested under compressive loading.

##### 4.2.1. Randomly distributed microcracks

The sample shown in Fig. 3 is subjected to uniaxial compression. The variations of the compliances  $\bar{S}_{22}$  (in the loading direction) and  $\bar{S}_{11}$  with density  $\rho$  are similar. Results for  $\bar{S}_{11}$  and  $\bar{S}_{33}$  are plotted in Fig. 10. Unlike the case of open cracks (important increase on compliance), very little increase is registered here. This is clearly due to the closure constraint imposed by compression on some microcracks.  $\bar{S}_{33}$  remains quite constant.

##### 4.2.2. Effect of microcracks inclined at $\pi/6$ from loading axis

The impact of crack orientation is also investigated. For this purpose, simulations were realized with arrays in which cracks are oriented at  $30^\circ$  from the loading axis (Fig. 11). The numerical results show significant anisotropy on the different compliances (Fig. 12). From the comparisons shown in this figure, we can conclude

that the results for  $\bar{S}_{11}$  and  $\bar{S}_{21}$  agree more with the SCM curve than with the NIC one (calculated from Ref. [10]). This suggests that microcrack interaction effects cannot be neglected for compressive loadings. Further investigations are needed to confirm this conclusion. Finally, some shielding effects are noted for  $\bar{S}_{22}$  and  $\bar{S}_{33}$ .

### 5. Concluding remarks

The aim of this numerical study is to investigate the impact of interactions on the effective stiffness of microcracked media by means of the displacement discontinuity method. A slight adaptation of the DDM (generation of random or non-random crack distribution, iterative algorithm for closed microcracks) is proposed. Since the unknown variables of DDM are COD on microcracks, the effective moduli calculation is straightforward. For tensile loadings, and when only crack – crack interactions are considered, the numerical results follow the non-interacting cracks approximation for a wide range of densities. This is due to the cancellation of amplification and shielding mechanisms associated with interactions where microcracks are randomly distributed. Moreover the numerical simulations showed that these conclusions hold for parallel distribution. Similar conclusions have been made by Kachanov [14] using a pseudo-traction method. It can be therefore concluded that, the non-interaction hypothesis will be sufficient for constitutive modeling. However, when microcrack – boundary interactions are also considered, the results indicate good agreement with the differential scheme. Under compressive loading, some microcracks are closed and subjected to friction. The results presented in this paper showed that for randomly distributed microcracks, friction effects decrease the impact of microcracks an effective compliance. For the studied parallel distribution, the results seem to be more in agreement

with the self-consistent method. Stress – induced anisotropy is also noticed. Current numerical investigations are in work on more complex distributions and on effective moduli in anisotropic media.

### References

- [1] Y. Belkacemi and R. Miguez, Crack path propagation with or without friction by displacement Discontinuity Method, European Mechanics Colloquium, Grenoble, (1988) p. 90.
- [2] Y. Bertaud, C. Fond and P. Brun, Mech. Res. Commun. 21 (E994) 525.
- [3] B. Budiansky and R.J. O'Connell, Int. J. Solids & Struc. 12 (1976) 81.
- [4] R.M. Christensen and K.H. Lo, J. Mech. Phys. Solids 27 (1979) 315.
- [5] R.M. Christensen, J. Mech. Phys. Solids, 38 (1990) 379.
- [6] S.L. Crouch, Int. J. Num. Meth. Engng., 10 (1976) 301.
- [7] S.L. Crouch and A.M. Starfield, Boundary Element Methods in Solid Mechanics (George Allen & Unwin, London, 1983).
- [8] Z. Hashin, J. Mech. Phys. Solids 36 (1988) 719.
- [9] R. Hill, J. Mech. Phys. Solids 15 (1966) 79.
- [10] M. Hori and S. Nemat-Nasser, J. Mech. Phys. Solids 31 (1983) 155.
- [11] J.W. Ju and X. Lee, J. Engng. Mech. ASCE 117 (1991) 1495.
- [12] J.W. Ju and K.W. Tseng, Int. J. Damage Mech. 1 (1992) 102.
- [13] M. Kachanov Int. J. Solids & Struc. 23 (1987) 23.
- [14] M. Kachanov, Appl. Mech. Rev. 45 (1992) 304.
- [15] D. Krajcinovic, Mechanics of Materials 8 (1989) 117.
- [16] X. Lee and J.W. Ju, J. Eng. Mech. ASCE 117 (1991) 1516.
- [17] Y.J. Lua, W.K. Liu and T. Belytschko, Int. J. Fract. 55 (1992) 321.
- [18] T. Mura, Micromechanics of Defects in Solids, 2nd Ed. (Nijhoff, Dordrecht, 1987).
- [19] S. Nemat-Nasser and M. Hori, Elastic solids with microdefects, in: Micromechanics and Inhomogeneity : T. Mura 65th Anniversary, ed. G.J. Weng, M. Taya and H. Abé, (Springer, Berlin, 1990) p. 297.
- [20] S. Nemat-Nasser and M. Hori, Micromechanics: Overall Properties of Heterogeneous Materials, (Elsevier, Amsterdam, 1993).
- [21] D. Sumarac and D. Krajcinovic, Mechanics of Materials 6 (1987) 39.
- [22] L. Vandamme, L. Ph.D. Dissertation, University of Toronto. Canada (1986).

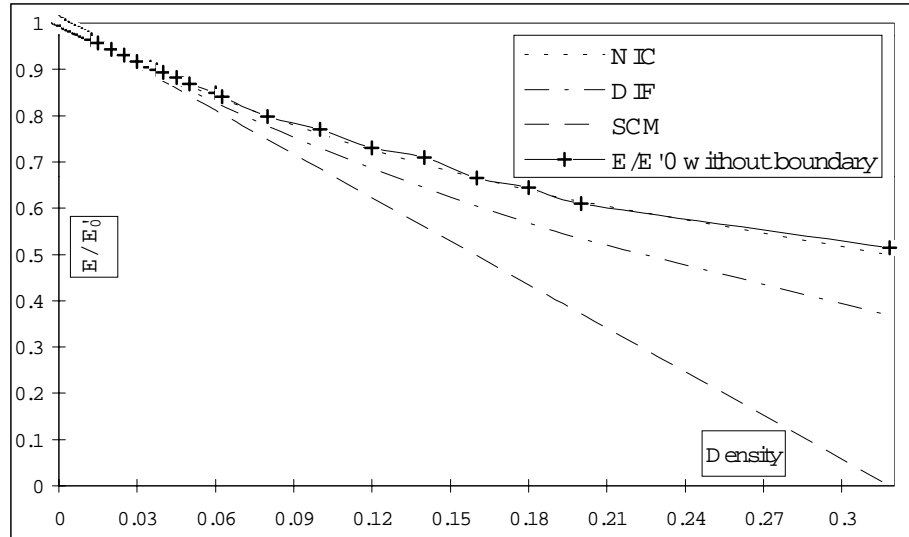


Fig. 4. Effective Young's modulus for randomly oriented microcracks. Crack size is constant: comparisons with the non-interacting cracks (NIC), self-consistent (SCM) and differential scheme (DIF).

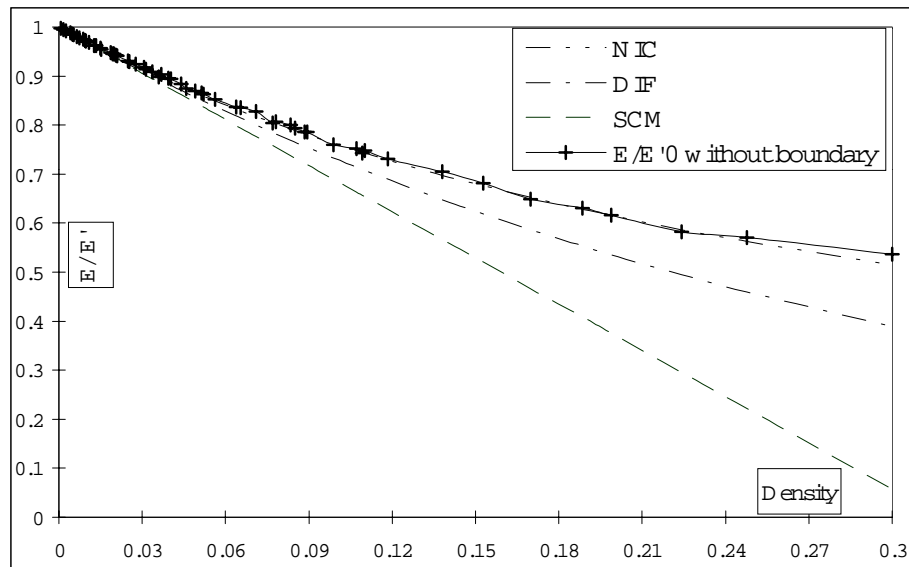


Fig. 5. Effective Young's modulus for full random distribution : comparisons with NIC, DIF and SCM.



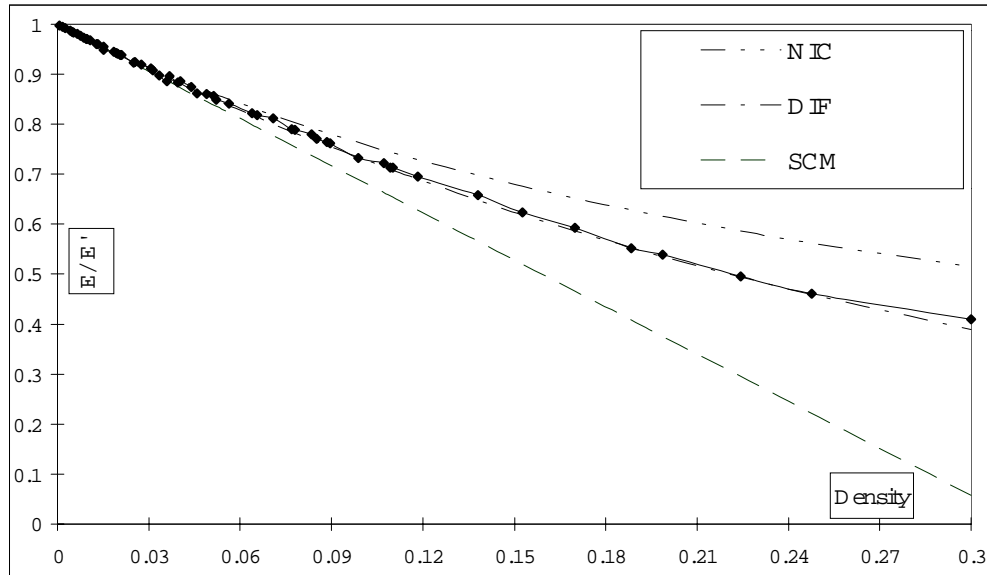


Fig. 6. Effect of microcrack-boundary interactions for random distribution : comparisons with NIC, DIF and SCM

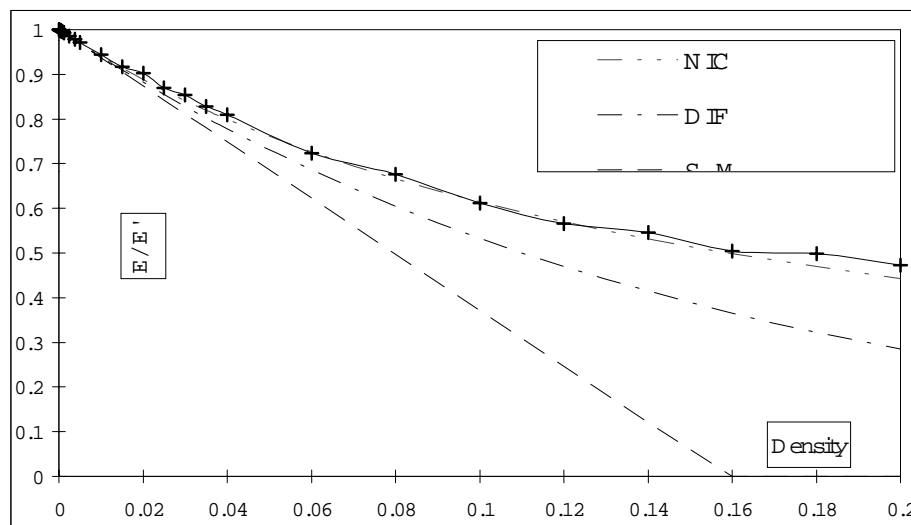


Fig. 8. Effective Young's modulus, for parallel microcracks : comparisons with the NIC, the DIF and the SCM schemes.

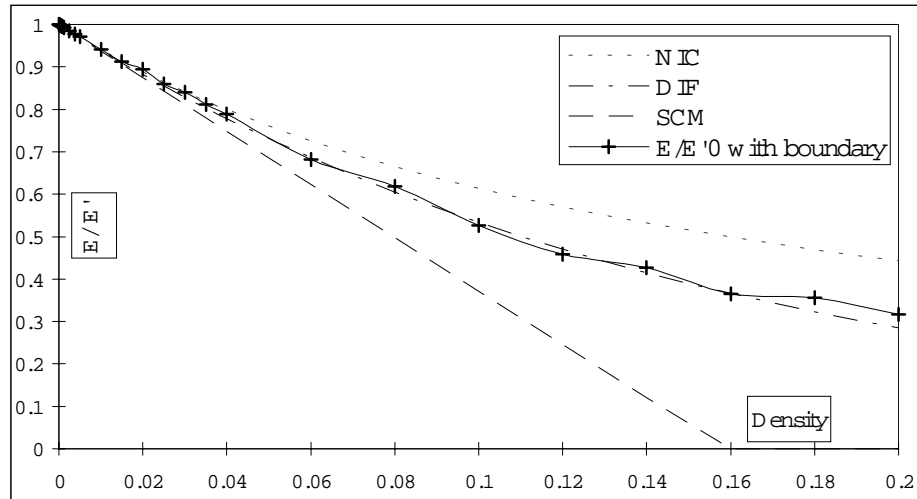


Fig. 9. Effect of microcrack – boundary interactions for parallel distribution : comparisons with the NIC, the DIF and the SCM schemes.

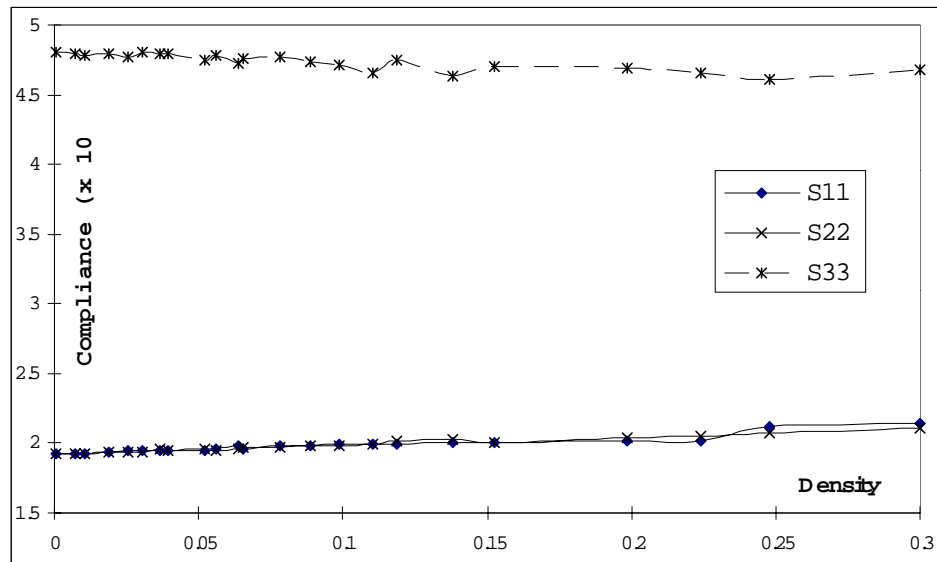


Fig. 10. Effective compliance for randomly microcracked medium under compressive loading ( $\mu = 0.5$ ).

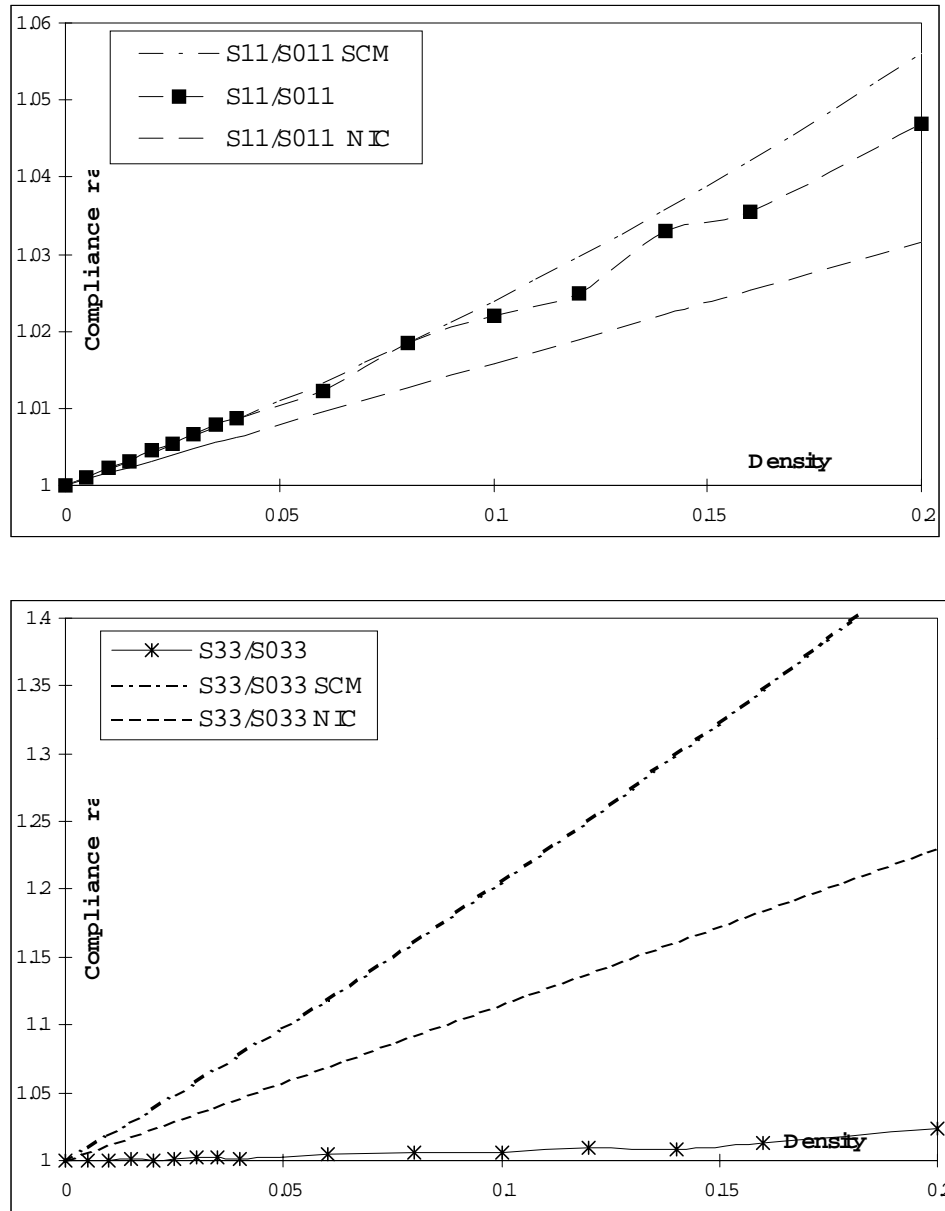


Fig. 12. Compressive loading. Effective compliance ratio for medium weakened by a set of parallel microcracks oriented at  $\pi/6$  from load direction ( $\mu = 0.5$ ):  $\bar{S}_{11}$ ,  $\bar{S}_{22}$ ,  $\bar{S}_{21}$ ,  $\bar{S}_{33}$ .

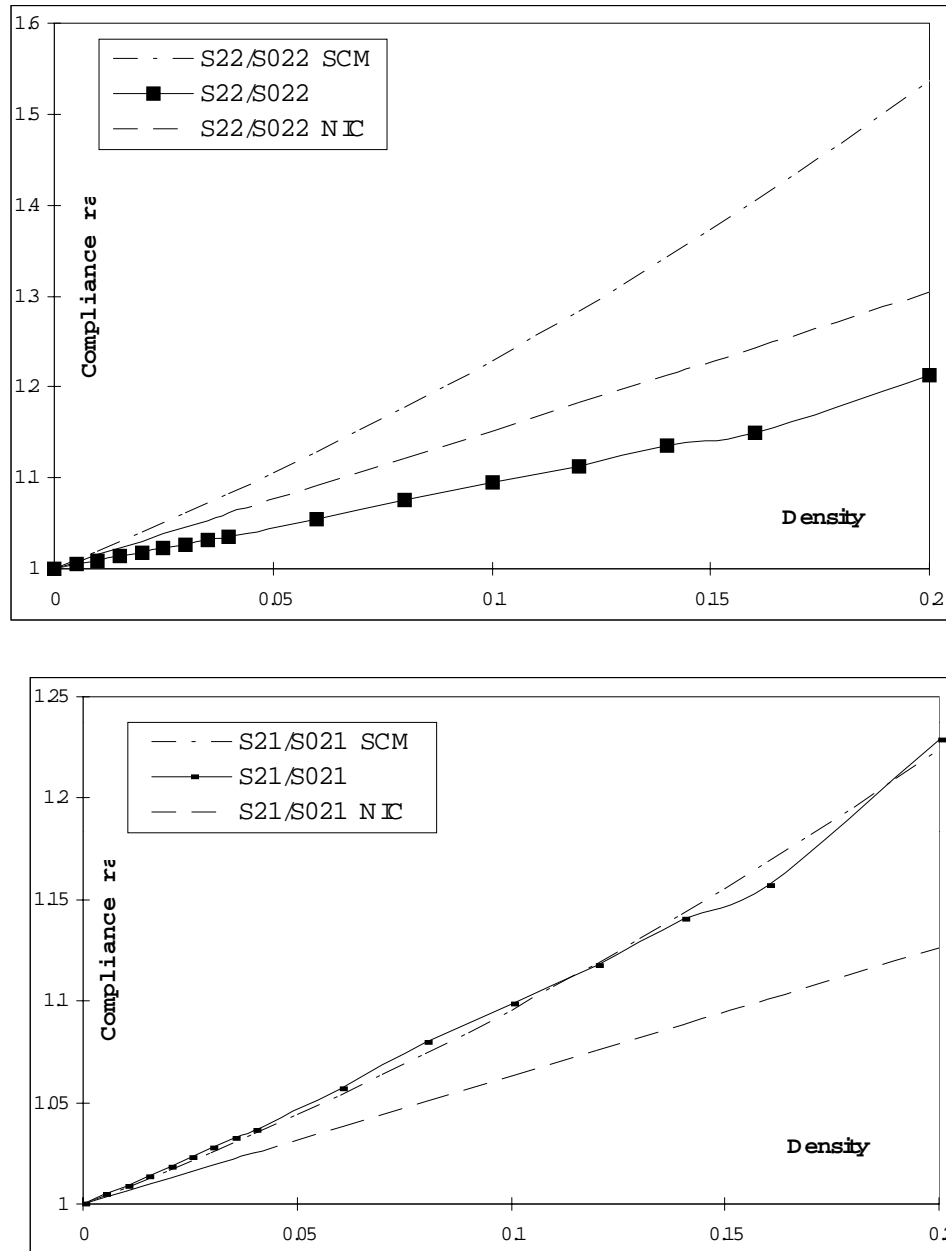


Fig. 12. (continued).